nature structural & molecular biology

β_2-microglobulin forms three-dimensional domain-swapped amyloid fibrils with disulfide linkages

Cong Liu[1–3], Michael R Sawaya[1–3] & David Eisenberg[1–3]

β_2-microglobulin (β_2m) is the light chain of the type I major histocompatibility complex. It deposits as amyloid fibrils within joints during long-term hemodialysis treatment. Despite the devastating effects of dialysis-related amyloidosis, full understanding of how fibrils form from soluble β_2m remains elusive. Here we show that β_2m can oligomerize and fibrillize via three-dimensional domain swapping. Isolating a covalently bound, domain-swapped dimer from β_2m oligomers on the pathway to fibrils, we were able to determine its crystal structure. The hinge loop that connects the swapped domain to the core domain includes the fibrillizing segment LSFSKD, whose atomic structure we also determined. The LSFSKD structure reveals a class 5 steric zipper, akin to other amyloid spines. The structures of the dimer and the zipper spine fit well into an atomic model for this fibrillar form of β_2m, which assembles slowly under physiological conditions.

A wide range of human pathologies are associated with the formation of amyloid fibrils from diverse polypeptide chains. More than 25 protein sequences have been found to be involved in protein deposition diseases, including Alzheimer's disease, dialysis-related amyloidosis and type 2 diabetes[1,2]. Despite the distinctly different sequences and tertiary structures of their precursor proteins, fibrils have extended β-sheet structures that show a common cross-β X-ray diffraction pattern[3]. In spite of recent insights into the atomic structure of amyloid-like fibrils revealed by crystallography[4,5], solid state NMR[6], EPR[7] and other methods, we lack full understanding of the molecular mechanisms that determine how soluble proteins assemble into well-organized fibrillar aggregates.

Oligomerization is regarded as a crucial step toward self-association of proteins into amyloid fibrils. In fact, oligomeric species as intermediates in fibrillogenesis are believed to be toxic in several types of amyloid-related neurodegenerative diseases[8,9]. Discovering the structures and molecular mechanisms of formation of these oligomers is crucial for identifying the fibrillation pathways and developing strategies to suppress amyloid-related diseases.

Recently, structural and biochemical studies of several amyloidogenic proteins have indicated that three-dimensional (3D) domain swapping is one of the common mechanisms for oligomerization[10–13]. 3D domain swapping is a general mechanism for protein oligomerization that works by converting an intramolecular interface in the monomer to an intermolecular interface between subunits in the oligomer[14]. More than 60 domain-swapped proteins have been structurally characterized. Growing evidence supports the hypothesis that domain swapping has diverse biological functions in oligomerization, fibril formation, conformational switching and allosteric regulation[15].

β_2-microglobulin (β_2m) is the light chain of the major histocompatibility class I (MHC I) complex. It contains 99 residues with one intramolecular disulfide bond[16]. Aggregation and deposition of wild-type β_2m occur in patients suffering from dialysis-related amyloidosis[17]. Under acidic conditions, β_2m self-assembles into amyloid-like fibrils spontaneously[18,19]. In contrast, under physiological conditions, additional factors such as copper[20], trifluoroethanol (TFE)[21] and collagen[22] are necessary for β_2m fibril formation[23]. A *cis-trans* isomerization of Pro32 or truncation of six N-terminal residues can facilitate the formation of β_2m fibrils[24,25]. The existence of several polymeric fibrillar forms of β_2m is suggested by observations that three different segments are involved in β_2m fibrillation: the aromatic-rich segment (residues 60–70)[26], the K3 segment (residues 20–41)[27] and the C-terminal segment (residues 83–89)[28]. Several β_2m oligomeric species have also been characterized[20,29,30], yet the linkage between oligomers and fibrils is unknown. Studies on the role of the disulfide bond in the fibrillation of β_2m indicate that β_2m does not form typical long-straight fibrils in the absence of the native intramolecular disulfide bond[31,32]. However, the propensity for β_2m fibrillation has not been reported under conditions in which disulfide exchange is possible.

In our research, we found that under physiological conditions, β_2m slowly condensed into covalently linked oligomers and eventually into worm-like protofilaments, and that the presence of reductants accelerated this process. We isolated a covalently linked dimer via the oligomeric mix and crystallized it. Its structure reveals a relatively rare but increasingly observed covalent domain swap, suggesting that the higher oligomers form via a runaway domain swap. Notably, the hinge loop connecting the swapped domain to the core domain turns out to be a segment predicted to be fiber forming. We were able to crystallize this segment and discovered that it indeed formed a steric

[1]University of California Los Angeles–United States Department of Energy Institute for Genomics and Proteomics, University of California, Los Angeles, Los Angeles, California, USA. [2]Howard Hughes Medical Institute, University of California, Los Angeles, Los Angeles, California, USA. [3]Molecular Biology Institute, University of California, Los Angeles, Los Angeles, California, USA. Correspondence should be addressed to D.E. (david@mbi.ucla.edu).

Received 15 March; accepted 16 September; published online 5 December 2010; doi:10.1038/nsmb.1948

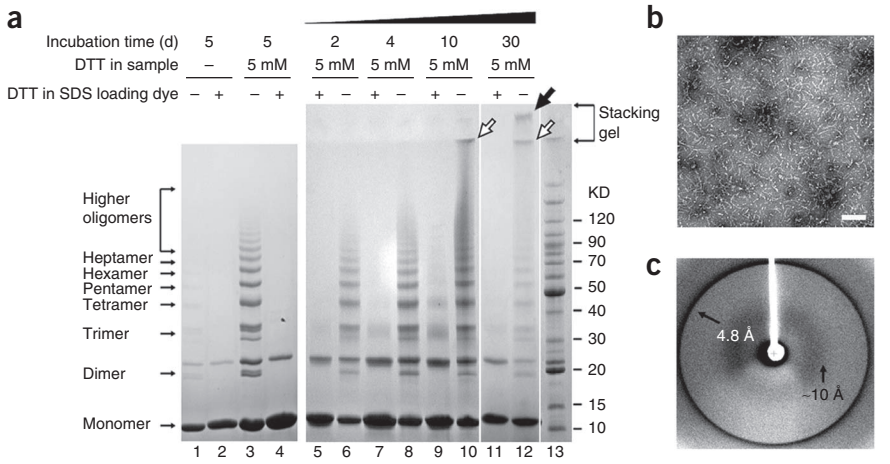

Figure 1 Characterization of β_2m oligomers. (**a**) SDS-PAGE of β_2m oligomerization under non-reducing and reducing conditions. Oligomerization started from monomeric β_2m with or without DTT agitated at 37 °C for various times. After 5 d, without DTT, oligomer ladders still formed (lane 1), but much slower than with DTT (lane 3). Over time, the disulfide-bridged oligomer ladders were observed (lane 6, 8, 10 and 12). After 10 d, even higher oligomers formed and remained at the boundary between the stacking gel and running gel (lanes 10 and 12, open arrows). After 30 d, protofilaments formed and were stuck in the loading well (lane 12, filled arrow). The oligomers were dissociated into monomers upon reduction in SDS loading buffer (+DTT) (lanes 2, 4, 5, 7, 9 and 11). Lane 13 is the BenchMark Protein Ladder (Invitrogen). The additional band above the dimer that exists in all β_2m samples is DTT resistant, unlike other oligomeric species. It is composed of β_2m, as found by amino acid sequencing, but the mechanism of its formation remains to be determined. (**b**) Electron micrograph showing the protofilaments formed in **a**. The scale bar is 200 nm. (**c**) Experimental fibril X-ray diffraction pattern of protofilaments visualized in **b**.

zipper, amyloid-like spine. The two atomic structures of the covalent, domain-swapped dimer and the steric zipper fit well into a fibril model, which is consistent with all of our biochemical and biophysical findings. Taking this rather complete picture of the formation of a β_2m protofibril together with the results of studies from other labs, we conclude that β_2m amyloid is a polymorphic mixture.

RESULTS

β_2m oligomers and protofilaments: formation and analysis

Recent studies indicate that Cu^{2+} is efficient in triggering β_2m oligomerization[33]. Dimers, tetramers and hexamers induced by Cu^{2+} have been well characterized, providing insights into early steps of β_2m aggregation[20,29,30]. In our work, we found that under physiological conditions, β_2m slowly condensed into covalently linked oligomers. By adding a reducing agent, we can accelerate the growth of the oligomers (**Fig. 1a**). The near-UV CD spectrum of oligomers showed a profile similar to that of the monomer, and the far-UV CD spectrum showed a β-rich structure, indicating that oligomers maintained a native-like structure rather than amorphous aggregates (**Supplementary Fig. 1**). After incubation with DTT at 37 °C for 2 d, the oligomers presented an ordered ladder on SDS-PAGE (**Fig. 1a**). With time, the sizes of the oligomers grew continuously. Higher oligomers that accumulated at the edge of the stacking gel formed after 10 d (**Fig. 1a**) and had no distinguishing morphology in EM images (data not shown). After 30 d, worm-like protofilaments appeared, as visualized by electron microscopy (**Fig. 1b**), and gave an X-ray diffraction pattern with ~4.8 Å and ~10 Å diffraction rings, characteristic of amyloid (**Fig. 1c**). On SDS-PAGE, the protofilaments remained in the loading well (**Fig. 1a**). These oligomers and protofilaments were resistant to SDS but dissociated to monomers in the presence of DTT in the loading buffer (**Fig. 1a**), indicating that their assembly is covalently mediated by intermolecular disulfide bonds.

Isolation and characterization of the β_2m dimer

β_2m was expressed in *Escherichia coli* and refolded to soluble protein. Addition of β-mercaptoethanol (βME) to β_2m in the dialysis buffer promoted the yield of dimer, trimer and tetramer, as identified by analytic size-exclusion chromatography (SEC) (**Fig. 2a**). After a few cycles of size exclusion, we could separate the dimer from the monomer and higher oligomers to high purity (**Fig. 2b**), but we failed to purify higher oligomeric species, owing to the minuscule amounts present. The purified dimer was SDS resistant and DTT sensitive on SDS-PAGE (**Fig. 2b**). CD spectra showed that the dimer has almost the same secondary structure as that of the monomer. Incubating the dimer with or without DTT resulted in the formation of the same oligomer ladders as were formed from monomeric β_2m (data not shown).

Crystal structure of the domain-swapped β_2m dimer

Crystallization and structure determination of monomeric, dimeric and hexameric species of β_2m have been reported[20,30,34]. The crystallographic structure of the reductant-triggered β_2m dimer we report here is strikingly different from the dimer and hexamer triggered by copper[20,30], indicating that different reagents can trigger different oligomerization pathways. In our structure, dimerization occurs via a relatively rare domain swap with covalent linkages. Identical 'domains'—β-strands E, F and G—are exchanged between the two subunits (**Fig. 3a**,**b**). Two interfaces between pairs of domains are created by this domain-swapping arrangement (**Fig. 3c**). One is termed the closed interface and is identical to the interface between domains in the monomer. The other is called the open interface and is a new β-sheet, formed by a hinge loop, that corresponds in sequence to loop L4 in monomeric β_2m (**Fig. 3a**,**c** and **Supplementary Fig. 2a**). The newly formed β-sheet links the two β_2m molecules in a twofold symmetric dimer and contributes to the stability of the dimer. The other dramatic feature of this domain-swapped

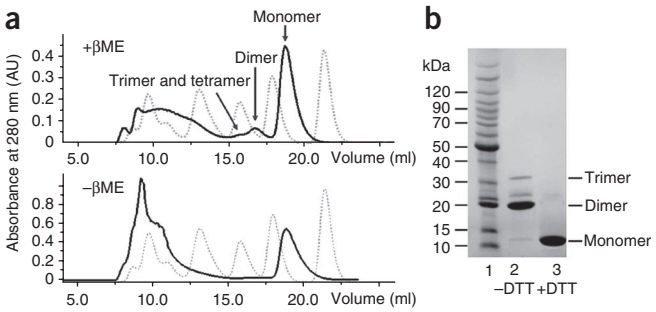

Figure 2 Refolding and purification of β_2m dimer. (**a**) Analytical size-exclusion chromatography elution profiles of β_2m after refolding. The dotted profiles show five molecular weight markers (Bio-Rad gel filtration standard). From right to left: vitamin B12 (M_r 1,350), equine myoglobin (M_r 17,000), chicken ovalbumin (M_r 44,000), bovine gamma globulin (M_r 158,000) and thyroglobulin (M_r 670,000). The solid profiles show β_2m refolding from inclusion bodies with or without βME. AU, absorbance units. (**b**) Purified dimer on SDS-PAGE. Lane 1, BenchMark Protein Ladder; lanes 2, 3, β_2m dimer in the absence or presence of DTT in SDS loading dye.

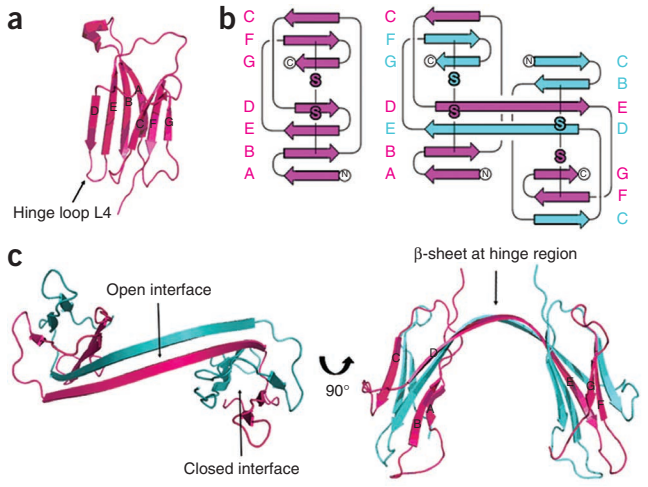

Figure 3 Structure of the domain-swapped β_2m dimer. (**a**) Ribbon diagram of the crystal structure of monomeric β_2m (PDB entry 1LDS[34]). (**b**) Topology diagrams of β_2m monomer and dimer. Intra- and intermolecular disulfide bonds are highlighted in the same color as the backbones. (**c**) Ribbon diagram of the crystal structure of β_2m domain-swapped dimer.

dimer is the rearrangement of the disulfide bonds. The intramolecular disulfide bond of β_2m re-forms as an intermolecular disulfide bond, thus covalently stabilizing the domain-swapped dimer (**Fig. 3b** and **Supplementary Fig. 2b**). The crystal structure provides structural evidence of how the intermolecular disulfide bond is formed and explains why the dimer is SDS resistant and DTT sensitive.

Compared to the existing β_2m structures, no major conformational changes are propagated in the β_2m molecule as a result of domain swapping (**Supplementary Fig. 3**). The superposition of β_2m in the domain-swapped dimer and in complex with the MHC (PDB ID code 1DUZ[35]) yields an r.m.s. deviation of 0.86 Å over 96 aligned pairs of α-carbons. Most of the small differences originate in the hinge loop. Comparison between β_2m in the domain-swapped dimer and the monomer (PDB ID code 1LDS[34]) yields a much larger r.m.s. deviation, 3.08 Å, but most of this deviation originates from a difference in conformations of a solvent-exposed loop spanning residues 12–21. When these residues are omitted from the calculation, the r.m.s. deviation is 0.58 Å. The difference in loop conformation is not attributed to domain swapping but to natural flexibility in this loop.

Proteolytic and mass spectrometric analyses of β_2m oligomers

Similar to the oligomers formed during refolding, the β_2m monomer also assembled into SDS-resistant and DTT-sensitive oligomers (**Fig. 1a**). This result suggests that oligomerization of the β_2m monomer also proceeds via 3D domain swapping. To test this hypothesis, we directly assessed the structural properties of oligomers using limited proteolysis and MALDI-TOF MS. We produced β_2m oligomers from both unlabeled and ^{15}N-labeled monomers and then subjected them to trypsin digestion. Accurate molecular masses of fragments digested by trypsin were measured by MALDI-TOF MS. (**Supplementary Fig. 4**). We focused mainly on one fragment comprising two peptides (D^{76}EYA**C**R^{81} and S^{20}NFLN**C**YVSGFHPSDIEVDLLK^{41}), linked via a disulfide bond formed by Cys25 and Cys80. The experimentally determined molecular mass of this fragment is 3,251.5 for unlabeled β_2m or 3,286.8 for ^{15}N-labeled β_2m. We then produced oligomers from a 1:1 molar ratio mixture of unlabeled and ^{15}N-labeled monomers and then carried out trypsin digestion. The disulfide bonded fragments gave four molecular masses instead of two. The appearance of two additional peaks with molecular masses of 3,260.9 and 3,279.0 indicated that the two peptides were from two different species of molecules (one from an unlabeled species and the other from a ^{15}N-labeled species) and were linked by intermolecular disulfide bonds. Rearrangement of the disulfide bond from intra- to intermolecular is the key indicator of domain-swapped assembly. Thus, it is conclusive that under our fibrillation condition, monomeric β_2m assembles into oligomers via domain swapping, and the oligomers are stabilized by intermolecular disulfide bonds, as showed in our atomic structure of the dimer. To further assess the role of intermolecular disulfide bonding in β_2m aggregation, we prepared a double C25S-C80S mutant (**Supplementary Methods**). The mutant was not able to form any kind of native-like oligomers or fibrils but formed only amorphous aggregates (**Supplementary Fig. 5**) at neutral pH, indicating the indispensability of the disulfide bonds in β_2m oligomerization and fibrillation.

Identification of amyloidogenic segments in the hinge loop

Studies of domain-swapped oligomerization have indicated that the new interaction formed by the hinge loop can stabilize the oligomeric state[36]. In a study of RNase A with Q_{10} inserted in the hinge loop[37], formation of a cross-β spine by the hinge loop contributes to stability of the fibril and accounts for the cross-β X-ray diffraction pattern. In many cases, hinge loops are crucial in mediating molecular assembly and participate in fibril core formation[37,38]. In order to identify the hinge loop segment forming the cross-β spine in β_2m fibrils, we conducted a systematic screen of the hinge loop. In the β_2m dimer, the hinge loop F^{56}SKDWS^{61} was located between β-strands D and E (**Fig. 3b,c**). We extended it to S^{52}DLSFSKDWSFYLL^{65} to cover half of βD and βE in case of potential small shifts of the hinge loop in higher oligomers compared with the dimer. We then screened segments for amyloid formation (**Fig. 4**). Each segment contained six residues

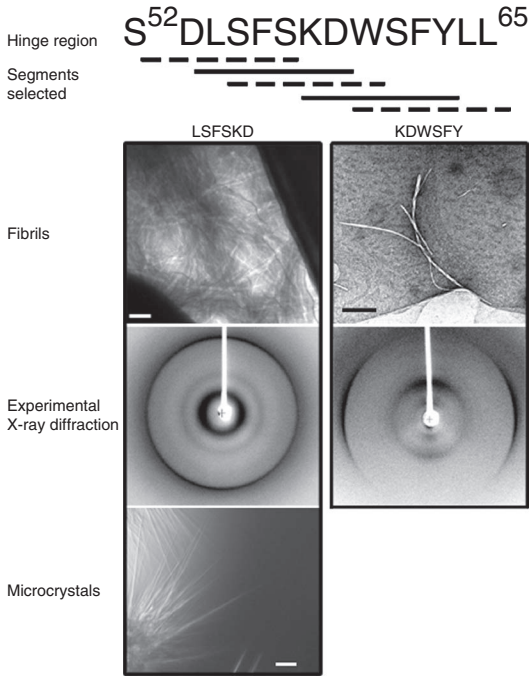

Figure 4 Systematic screening for amyloidogenic segments in the hinge loop (residues 52–65). Five segments were selected and synthesized. LSFSKD and KDWSFY in solid lines formed fibrils, and LSFSKD also formed microcrystals. The scale bars are 100 nm for electron microscopy (fibrils) and 50 μm for light microscopy (microcrystals). The experimental X-ray diffraction images show a typical cross-β fibril diffraction pattern.

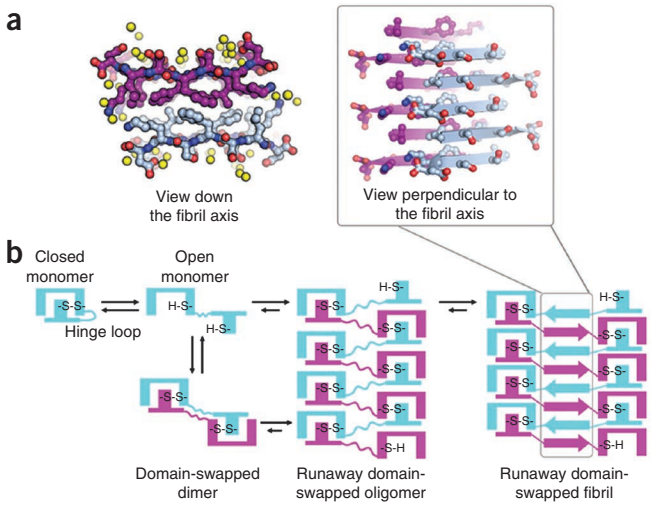

Figure 5 Crystal structure of segment LSFSKD and schematics for β_2m fibrillation. (**a**) Atomic structure of hinge loop segment LSFSKD. Yellow spheres represent water molecules. The backbone of one sheet is magenta, and the backbone of the other sheet is blue. The interdigitated side chains between adjacent β-sheets form a dry interface, as shown by the projection down the fibril axis on the left. The LSFSKD structure is a typical steric zipper structure, belonging to class 5 (ref. 5). (**b**) Schematic model for β_2m fibrillation via domain swapping. Upon reduction of the intramolecular disulfide bond, the β_2m monomer can assemble to 'closed-ended' oligomers, such as the dimer characterized in this work, or 'open-ended' runaway domain-swapped oligomers. Each subunit is colored in either blue or magenta. The formation of intermolecular disulfide bonds stabilizes the domain-swapped oligomers. The self-association of hinge loops into a zipper spine accomplishes the transformation from oligomers into fibrils.

and was incubated at a series of conditions (see Online Methods) for fibril formation. After 3 weeks, only LSFSKD and KDWSFY formed fibrils. LSFSKD fibrils tended to aggregate into clusters, whereas the KDWSFY fibrils had more rigid morphology (**Fig. 4**). The X-ray fibril diffraction images of these two segments showed typical cross-β diffraction patterns. Thus, LSFSKD and KDWSFY segments were identified as potential candidates for forming the cross-β spine in domain-swapped β_2m fibrillation.

Atomic structure of the amyloidogenic segment LSFSKD

Previous studies of short peptide segments showed the relationship between fibrils and microcrystals and revealed that the crystal structures of the segments are related to structures of the fibrils formed by the same segments[5]. In our study, in order to discover the atomic-level structure of the hinge loop in the spine of the 3D domain-swapped fibrils, we crystallized and determined the crystal structure of LSFSKD (**Fig. 5a** and **Supplementary Fig. 2c**). Each LSFSKD molecule forms hydrogen bonds with the identical segments above and below, within an extended antiparallel β-sheet along the fibril axis. A pair of sheets in the crystal forms a tightly interdigitated dry interface and extended the whole length of the fibril-like structure into needle-like microcrystals. The strands in the neighboring sheet are antiparallel, and sheets pack with the same surface adjacent to one another. Each sheet is related to its mate by a twofold screw axis that is parallel to the needle crystal. The shape complementarity (Sc) of the sheet interface is 0.73, and the area buried is 470 Å^2, contributed primarily by the three side chains (Leu54, Phe56 and Lys58) of two molecules. These features indicate that LSFSKD forms a typical amyloid spine, consisting of a class 5 steric zipper[5]. The hydrophobic interface between the two sheets is contributed by leucine and phenylalanine. Recent studies show that grafting an 'FXL' cluster (X represents any residue) onto a large β-sheet protein causes protein self-assembly via formation of a cross-β architecture[39], which is similar to the LSFSKD steric zipper structure, indicating a strong potential of the LSFSKD segment to drive self-association. We infer that for full-length β_2m, the hinge loop mediates molecular assembly via domain swapping. The zipper structure of LSFSKD shows how the LSFSKD segment provides spine formation. From this steric zipper structure, it is plausible to build a runaway domain-swapped, zipper-spine atomic model, as discussed below.

DISCUSSION

Runaway 3D domain-swapped, zipper-spine β_2m fibril model

Our determination of the crystal structure of LSFSKD illustrates how the cross-β spine of domain-swapped β_2m may form. A recent study reinforced the notion that the cross-β structure represents the common spine for amyloid fibrils, based on the authors' systematic comparison of fibril diffraction patterns with model simulations[40]. For fibril assembly from native-like proteins, a newly formed cross-β spine is necessary and sufficient to provide the common cross-β diffraction signature. Previous studies regarding the fibril formation via domain swapping show that the hinge loop is crucial in forming the cross-β spine[15,37,38]. In our β_2m studies, we experimentally identified two natural amyloidogenic segments within the hinge loop of domain-swapped β_2m. Either of them is capable of forming the core of the fibril, but in our crystal structure of the domain-swapped dimer, neither one precisely pairs to interact with the identical segment in the hinge loop (**Supplementary Fig. 2a**). However, as the oligomer grows, the loop regions between swapped domains can slide slightly, to adapt to the packing geometry of globular protomers. Given the positions of the segments in the hinge loop, LSFSKD is the segment more likely to form a face-to-face steric zipper and compose the β-spine of the β_2m fibril. KDWSFY is close to β-strand E, which hinders its exposure and self-assembly during β_2m aggregation.

Based on the atomic structures of the domain-swapped dimer and the steric zipper, we built a domain-swapped zipper-spine model of a β_2m fibril (**Supplementary Fig. 6a–c** and **Supplementary Methods**), which is consistent with all of our biochemical and biophysical findings. The model takes its spine directly from the LSFSKD crystal structure (residues 53–58 of human β_2m) (**Fig. 5a**). β_2m molecules that assemble via runaway domain swapping are covalently linked by intermolecular disulfide bonds. The calculated and observed X-ray diffraction patterns agree in relative intensity and Bragg angle for the strongest reflections (**Supplementary Fig. 6d** and **Supplementary Methods**). The additional, weaker reflections present in the calculated pattern are absent from the observed diffraction pattern, perhaps because of disorder in the fiber. That is, the level of agreement is what is expected to support our model. Our domain-swapped zipper-spine model incorporates runaway 3D domain swapping that contributes to the globular and native-like assembly of the fibril. Also, the steric zipper formed by hinge loops forms the fibril spine and gives rise to the signature cross-β diffraction pattern.

We note that a limitation of our model is that it does not explain the observed, curved morphology of the β_2m protofilaments in the EM images. The fibril model was generated using perfect screw axis symmetry. It lends the appearance of being perfectly ordered and rigid. However, we do not mean to imply that the fibril maintains such perfect symmetry and rigidity. There are some restrictions on the flexibility of the zipper spine because it has a specific and extensive

Table 1 Comparison of proposed β_2m fibril models

Fibril model	Fibrillation condition	Morphology	β_2m conformation	Ref.
β-strands stacked in parallel, in register	25 mM sodium phosphate buffer, pH 2.5	Long-straight	Highly non-native	48
Zipper spine formed via C-terminal segment	0.2 M NaCl, 25 mM phosphate, pH 2.0	Long-straight	Native-like	28
Head-to-head, tail-to-tail, cross-β core formed via β-strands A, B, E & D	0.2 mM Cu^{2+}, 25 mM MOPS, 0.2 M $KC_2H_3O_2$, 0.5 M urea, pH 7.4	Fibrous	Native-like	20,33
3D domain swapping with S-S linkage and zipper spine formed by the hinge loop	20 mM Tris-HCl, 5 mM DTT, pH 8.0	Worm-like	Native-like	This work

hydrogen bonding pattern, but the globular domains arranged around the zipper spine may take different orientations. They are not connected to neighboring domains by a rigid hydrogen bonding network but are simply tethered to the zipper by a hinge loop. The possibility for different arrangements of the globular domains could contribute to the degree of curvature observed in the electron micrograph. It is also possible that the worm-like protofilament seen under EM is an intermediate, which may anneal into straighter fibrils.

β_2m fibrillation via domain swapping with S-S rearrangement

Though evidence has accumulated that 3D domain swapping plays a role in some cases of amyloidogenesis[10–13,15,37], direct experimental support for this, and understanding of the conversion process, have been limited. Lingering questions include what triggers the assembly of monomers to oligomers by domain swapping, and what stabilizes the fibrils. In the case of β_2m fibrillation via 3D domain swapping with disulfide linkages, we propose a molecular mechanism to answer these questions (**Fig. 5b**). The process is initiated when a small amount of open-form monomer is generated by breakage of the intramolecular disulfide bond. Then, by thiol-disulfide exchange, the open monomer is converted to a domain-swapped dimer and higher oligomers. The gain of intermolecular disulfide bonds covalently stabilizes the domain-swapped oligomers. The thiol-disulfide exchange we postulate to start the process is known to occur in biological tissues and environments considered to be oxidizing (such as blood, where β_2m fibrils form) as well as reducing[41]. Disulfide-bond rearrangement has also been observed in the aggregation of cystatin C and the human prion protein[10,12,38,42]. As the covalent polymer grows, the new β-sheet interactions formed in the hinge loops cause them to align into a cross-β zipper spine that forms the central spine of the fibril. The zipper spine formation bridges the gap between oligomers and fibrils. To illustrate the existence and importance of the zipper spine, we also built a domain-swapped model without a zipper spine (**Supplementary Fig. 7a**,**b**). Instead of the cross-β signature, the simulated diffraction pattern of this model contains several rings spreading out from low to high resolution, which is totally different from the experimental diffraction pattern (**Supplementary Fig. 7c**). This result shows that the association of hinge loops into the zipper spine is an essential step toward β_2m fibril maturation.

Notice that to form fibrils from an oligomeric state, no large conformational change is necessary; rather, the β-strands in hinge loops associate into the cross-β spine. This means that the energy barrier between oligomers and fibrils is not large, as is expected for on-pathway oligomers. The mechanism we propose is also related to a more general mechanism for domain-swapped fibril formation in the absence of a disulfide linkage. The steps in fibril formation would be the same, except the requirement for disulfide-bond breakage and re-formation would be omitted. Omission of the disulfide bond would lower the barrier to fibril formation and disassembly.

Figure 1a shows a subtle feature that is consistent with our model for fibril formation: doublet bands for the dimeric and trimeric species on the SDS-PAGE gel. Based on the mechanism proposed above, oligomers may have two major conformations. One is a closed form in which all cysteines form intermolecular disulfide bonds. The other is an open form in which the cysteines on both termini are free to accept more β_2m molecules for fibril elongation. The upper band in the doublet most likely corresponds to the open form because it is more elongated than the cyclized closed form. As the oligomers grow, the terminal β_2m molecules are farther apart from each other, and the probability of forming a closed, cyclized oligomer is lower. The population of the closed form is therefore too small to see in higher oligomers. The same phenomenon was also observed and well characterized in the T7 endonuclease I domain-swapped oligomerization[11].

β_2m amyloid polymorphism

Heterogeneity is a common property of amyloid fibrils, which reflects polymorphism at the molecular level[43]. Recent studies show that, unlike those for the folding of soluble proteins, energy landscapes of amyloid assemblies contain multiple minima that can be reached through different fibrillation pathways that start from the same initial

Table 2 Statistics of crystallographic data collection and atomic refinement

	Domain-swapped β_2m dimer	Segment LSFSKD
Data collection		
Space group	$P2_1$	$P2_1$
Cell dimensions		
a, *b*, *c* (Å)	59.72, 29.16, 67.72	9.43, 21.48, 45.73
α, *β*, *γ* (°)	90.0, 97.49, 90.0	90.0, 90.0, 90.0
Resolution (Å)	50–2.19 (2.23–2.19)	80–1.8 (1.86–1.8)
R_{merge} (%)	5.7 (20.5)	11.8 (50.1)
$I / \sigma I$	14.0 (6.6)	20.1 (4.7)
Completeness (%)	99.3 (99.1)	93.7 (82.0)
Redundancy	3.6 (3.4)	3.8 (3.2)
Refinement		
Resolution (Å)	2.3	1.8
No. reflections	10,065	1,499
R_{work} / R_{free} (%)	21.9 / 26.7	21.6 / 24.1[a]
No. atoms		
Protein	1,605	205
Water	33	17
B-factors (Å^2)		
Protein	31.0	16.1
Water	37.8	27.5
R.m.s. deviations		
Bond lengths (Å)	0.016	0.006
Bond angles (°)	1.595	0.979

Values in parentheses are for highest-resolution shell. One crystal was used for β_2m dimer data collection. Two crystals were used to obtain the peptide dataset.
[a]Ten percent of the reflections were withheld for the calculation of R_{free}, a cross-validation tool. Compared to macromolecular crystallography, the R_{free} reported here has reduced significance owing to the reduced number of reflections accompanying a relatively smaller unit cell.

state[44]. Physicochemical environment plays a crucial role in directing the fibrillation pathways. Different fibril architectures formed by the same protein have been elucidated by solid-state NMR, EM and other methods[45,46]. Recent structural studies on polymorphic short segments at an atomic level also provide a steric zipper mechanism for amyloid and prion polymorphism, including packing polymorphism, segmental polymorphism and single-chain registration polymorphism[47].

In vitro studies on β_2m fibrillation show that β_2m forms fibrils with various morphology under various conditions[22,30,33,48–50]. Several β_2m fibril models are proposed based on the experimental evidence obtained from a specific fibrillation condition and fibril form (**Table 1**). The variation of the models reflects the polymorphism of β_2m fibrils. The *in vivo* environment for β_2m is even more complicated and variable than that in *in vitro* experiments. Actually, β_2m amyloid fibrils extracted from patient tissue are heterogeneous and can be sorted into several fractions on the basis of their aqueous solubility, apparently because they have different fibril architectures[51,52]. Combining the *in vitro* and *in vivo* observations, it appears that β_2m molecular assembly may involve various protein segments and depend upon the local environment, and probably leads to various aggregation pathways.

Physiological relevance of domain-swapped β_2m fibrillation

β_2m forms domain-swapped oligomers under physiological conditions (**Fig. 1a**). However, due to the high energy barrier for breaking intramolecular disulfide bonds, this oligomerization develops very slowly, on a timescale of months. Because fibrils are elongated stacked oligomers, domain-swapped fibrils would be expected to take longer to form. In dialysis-related amyloidosis patients, β_2m amyloid fibrils are generally detected after several years of dialysis treatment[17] and the concentration of β_2m can increase by up to 60-fold in the serum compared with the level under normal kidney function (0.09–0.17 μM)[53]. Considering the specific environment within osteoarticular tissues and the uremic environment caused by decreased kidney function[23], local concentrations of β_2m can be even higher. Also, the worm-like appearance of our β_2m disulfide-linked protofilaments is similar to the appearance of *ex vivo* β_2m fibers with a 'curvilinear configuration' seen in another study[54]. In terms of environment, timescale, protein concentration and fibril morphology, β_2m fibrillation *in vivo* is comparable to the 3D domain-swapped β_2m fibrillation *in vitro*, suggesting that the 3D domain-swapped aggregation with disulfide linkages and a zipper spine may play a role in β_2m-related, dialysis-related amyloidosis.

METHODS

Methods and any associated references are available in the online version of the paper at http://www.nature.com/nsmb/.

Accession codes. Protein Data Bank: Coordinates and structure factors for domain-swapped β_2m dimer and amyloidogenic segment LSFSKD have been deposited with accession codes 3LOW and 3LOZ, respectively.

Note: Supplementary information is available on the Nature Structural & Molecular Biology website.

ACKNOWLEDGMENTS

We thank the Northeastern Collaborative Access Team facility at the Advanced Photon Source at Argonne National Laboratory for beam time and collection assistance, and S. Radford, M. Bennett and Z. Guo for discussion. This work was supported by the US National Institutes of Health, the US Department of Energy Biological and Environmental Research program and the Howard Hughes Medical Institute.

AUTHOR CONTRIBUTIONS

C.L. designed the research, with advice from D.E., and carried out all the experiments; M.R.S. calculated and built the fibril models; C.L. wrote the paper; all authors discussed the results and revised the manuscript; D.E. supervised the work.

COMPETING FINANCIAL INTERESTS

The authors declare no competing financial interests.

Published online at http://www.nature.com/nsmb/.
Reprints and permissions information is available online at http://npg.nature.com/reprintsandpermissions/.

1. Westermark, P. *et al.* Amyloid: toward terminology clarification. Report from the Nomenclature Committee of the International Society of Amyloidosis. *Amyloid* **12**, 1–4 (2005).
2. Chiti, F. & Dobson, C.M. Protein misfolding, functional amyloid, and human disease. *Annu. Rev. Biochem.* **75**, 333–366 (2006).
3. Makin, O.S. & Serpell, L.C. Structures for amyloid fibrils. *FEBS J.* **272**, 5950–5961 (2005).
4. Nelson, R. *et al.* Structure of the cross-β spine of amyloid-like fibrils. *Nature* **435**, 773–778 (2005).
5. Sawaya, M.R. *et al.* Atomic structures of amyloid cross-β spines reveal varied steric zippers. *Nature* **447**, 453–457 (2007).
6. Tycko, R. Molecular structure of amyloid fibrils: insights from solid-state NMR. *Q. Rev. Biophys.* **39**, 1–55 (2006).
7. Margittai, M. & Langen, R. Fibrils with parallel in-register structure constitute a major class of amyloid fibrils: molecular insights from electron paramagnetic resonance spectroscopy. *Q. Rev. Biophys.* **41**, 265–297 (2008).
8. Glabe, C.G. Common mechanisms of amyloid oligomer pathogenesis in degenerative disease. *Neurobiol. Aging* **27**, 570–575 (2006).
9. Bucciantini, M. *et al.* Inherent toxicity of aggregates implies a common mechanism for protein misfolding diseases. *Nature* **416**, 507–511 (2002).
10. Wahlbom, M. *et al.* Fibrillogenic oligomers of human cystatin C are formed by propagated domain swapping. *J. Biol. Chem.* **282**, 18318–18326 (2007).
11. Guo, Z. & Eisenberg, D. Runaway domain swapping in amyloid-like fibrils of T7 endonuclease I. *Proc. Natl. Acad. Sci. USA* **103**, 8042–8047 (2006).
12. Knaus, K.J. *et al.* Crystal structure of the human prion protein reveals a mechanism for oligomerization. *Nat. Struct. Biol.* **8**, 770–774 (2001).
13. Janowski, R. *et al.* Human cystatin C, an amyloidogenic protein, dimerizes through three-dimensional domain swapping. *Nat. Struct. Biol.* **8**, 316–320 (2001).
14. Gronenborn, A.M. Protein acrobatics in pairs—dimerization via domain swapping. *Curr. Opin. Struct. Biol.* **19**, 39–49 (2009).
15. Bennett, M.J., Sawaya, M.R. & Eisenberg, D. Deposition diseases and 3D domain swapping. *Structure* **14**, 811–824 (2006).
16. Becker, J.W. & Reeke, G.N. Jr. Three-dimensional structure of β_2-microglobulin. *Proc. Natl. Acad. Sci. USA* **82**, 4225–4229 (1985).
17. Campistol, J.M. *et al.* Polymerization of normal and intact β_2-microglobulin as the amyloidogenic protein in dialysis-amyloidosis. *Kidney Int.* **50**, 1262–1267 (1996).
18. McParland, V.J., Kalverda, A.P., Homans, S.W. & Radford, S.E. Structural properties of an amyloid precursor of β_2-microglobulin. *Nat. Struct. Biol.* **9**, 326–331 (2002).
19. McParland, V.J. *et al.* Partially unfolded states of β_2-microglobulin and amyloid formation in vitro. *Biochemistry* **39**, 8735–8746 (2000).
20. Eakin, C.M., Berman, A.J. & Miranker, A.D. A native to amyloidogenic transition regulated by a backbone trigger. *Nat. Struct. Mol. Biol.* **13**, 202–208 (2006).
21. Yamaguchi, K., Naiki, H. & Goto, Y. Mechanism by which the amyloid-like fibrils of a β_2-microglobulin fragment are induced by fluorine-substituted alcohols. *J. Mol. Biol.* **363**, 279–288 (2006).
22. Myers, S.L. *et al.* A systematic study of the effect of physiological factors on β_2-microglobulin amyloid formation at neutral pH. *Biochemistry* **45**, 2311–2321 (2006).
23. Heegaard, N.H. β_2-microglobulin: from physiology to amyloidosis. *Amyloid* **16**, 151–173 (2009).
24. Jahn, T.R., Parker, M.J., Homans, S.W. & Radford, S.E. Amyloid formation under physiological conditions proceeds via a native-like folding intermediate. *Nat. Struct. Mol. Biol.* **13**, 195–201 (2006).
25. Esposito, G. *et al.* Removal of the N-terminal hexapeptide from human β_2-microglobulin facilitates protein aggregation and fibril formation. *Protein Sci.* **9**, 831–845 (2000).
26. Platt, G.W., Routledge, K.E., Homans, S.W. & Radford, S.E. Fibril growth kinetics reveal a region of β_2-microglobulin important for nucleation and elongation of aggregation. *J. Mol. Biol.* **378**, 251–263 (2008).
27. Iwata, K. *et al.* 3D structure of amyloid protofilaments of β_2-microglobulin fragment probed by solid-state NMR. *Proc. Natl. Acad. Sci. USA* **103**, 18119–18124 (2006).
28. Ivanova, M.I., Sawaya, M.R., Gingery, M., Attinger, A. & Eisenberg, D. An amyloid-forming segment of β_2-microglobulin suggests a molecular model for the fibril. *Proc. Natl. Acad. Sci. USA* **101**, 10584–10589 (2004).

29. Blaho, D.V. & Miranker, A.D. Delineating the conformational elements responsible for Cu2+-induced oligomerization of β_2-microglobulin. *Biochemistry* **48**, 6610–6617 (2009).
30. Calabrese, M.F., Eakin, C.M., Wang, J.M. & Miranker, A.D. A regulatable switch mediates self-association in an immunoglobulin fold. *Nat. Struct. Mol. Biol.* **15**, 965–971 (2008).
31. Katou, H. *et al.* The role of disulfide bond in the amyloidogenic state of β_2-microglobulin studied by heteronuclear NMR. *Protein Sci.* **11**, 2218–2229 (2002).
32. Smith, D.P. & Radford, S.E. Role of the single disulphide bond of β_2-microglobulin in amyloidosis *in vitro*. *Protein Sci.* **10**, 1775–1784 (2001).
33. Eakin, C.M., Attenello, F.J., Morgan, C.J. & Miranker, A.D. Oligomeric assembly of native-like precursors precedes amyloid formation by β_2-microglobulin. *Biochemistry* **43**, 7808–7815 (2004).
34. Trinh, C.H., Smith, D.P., Kalverda, A.P., Phillips, S.E. & Radford, S.E. Crystal structure of monomeric human β_2-microglobulin reveals clues to its amyloidogenic properties. *Proc. Natl. Acad. Sci. USA* **99**, 9771–9776 (2002).
35. Khan, A.R., Baker, B.M., Ghosh, P., Biddison, W.E. & Wiley, D.C. The structure and stability of an HLA-A*0201/octameric tax peptide complex with an empty conserved peptide-N-terminal binding site. *J. Immunol.* **164**, 6398–6405 (2000).
36. Rousseau, F., Schymkowitz, J.W., Wilkinson, H.R. & Itzhaki, L.S. Three-dimensional domain swapping in p13suc1 occurs in the unfolded state and is controlled by conserved proline residues. *Proc. Natl. Acad. Sci. USA* **98**, 5596–5601 (2001).
37. Sambashivan, S., Liu, Y., Sawaya, M.R., Gingery, M. & Eisenberg, D. Amyloid-like fibrils of ribonuclease A with three-dimensional domain-swapped and native-like structure. *Nature* **437**, 266–269 (2005).
38. Lee, S. & Eisenberg, D. Seeded conversion of recombinant prion protein to a disulfide-bonded oligomer by a reduction-oxidation process. *Nat. Struct. Biol.* **10**, 725–730 (2003).
39. Biancalana, M., Makabe, K. & Koide, S. Minimalist design of water-soluble cross-β architecture. *Proc. Natl. Acad. Sci. USA* **107**, 3469–3474 (2010).
40. Jahn, T.R. *et al.* The common architecture of cross-β amyloid. *J. Mol. Biol.* **395**, 717–727 (2010).
41. Hogg, P.J. Disulfide bonds as switches for protein function. *Trends Biochem. Sci.* **28**, 210–214 (2003).
42. Nilsson, M. *et al.* Prevention of domain swapping inhibits dimerization and amyloid fibril formation of cystatin C: use of engineered disulfide bridges, antibodies, and carboxymethylpapain to stabilize the monomeric form of cystatin C. *J. Biol. Chem.* **279**, 24236–24245 (2004).
43. Fändrich, M., Meinhardt, J. & Grigorieff, N. Structural polymorphism of Alzheimer Aβ and other amyloid fibrils. *Prion* **3**, 89–93 (2009).
44. Kodali, R. & Wetzel, R. Polymorphism in the intermediates and products of amyloid assembly. *Curr. Opin. Struct. Biol.* **17**, 48–57 (2007).
45. Goldsbury, C.S. *et al.* Polymorphic fibrillar assembly of human amylin. *J. Struct. Biol.* **119**, 17–27 (1997).
46. Paravastu, A.K., Leapman, R.D., Yau, W.M. & Tycko, R. Molecular structural basis for polymorphism in Alzheimer's β-amyloid fibrils. *Proc. Natl. Acad. Sci. USA* **105**, 18349–18354 (2008).
47. Wiltzius, J.J. *et al.* Molecular mechanisms for protein-encoded inheritance. *Nat. Struct. Mol. Biol.* **16**, 973–978 (2009).
48. Ladner, C.L. *et al.* Stacked sets of parallel, in-register β-strands of β_2-microglobulin in amyloid fibrils revealed by site-directed spin labeling and chemical labeling. *J. Biol. Chem.* **285**, 17137–17147 (2010).
49. Yamamoto, K. *et al.* Thiol compounds inhibit the formation of amyloid fibrils by β_2-microglobulin at neutral pH. *J. Mol. Biol.* **376**, 258–268 (2008).
50. Chen, Y. & Dokholyan, N.V. A single disulfide bond differentiates aggregation pathways of β_2-microglobulin. *J. Mol. Biol.* **354**, 473–482 (2005).
51. Stoppini, M. *et al.* Proteomics of β_2-microglobulin amyloid fibrils. *Biochim. Biophys. Acta* **1753**, 23–33 (2005).
52. Bellotti, V. β_2-microglobulin can be refolded into a native state from *ex vivo* amyloid fibrils. *Eur. J. Biochem.* **258**, 61–67 (1998).
53. Platt, G.W. & Radford, S.E. Glimpses of the molecular mechanisms of β_2-microglobulin fibril formation *in vitro*: aggregation on a complex energy landscape. *FEBS Lett.* **583**, 2623–2629 (2009).
54. Gorevic, P.D. *et al.* Beta-2 microglobulin is an amyloidogenic protein in man. *J. Clin. Invest.* **76**, 2425–2429 (1985).

ONLINE METHODS

Cloning, expression and purification. Wild-type β_2m was expressed in *E. coli* and β_2m monomer was purified from inclusion bodies via refolding as described previously[28]. For producing β_2m dimer, 1 mM β-mercaptoethanol (βME) was maintained in the dialysis buffer during refolding. After refolding, β_2m was purified by using Superdex 200 (GE Healthcare) in 20 mM Tris-HCl, pH 8.0. The MW of β_2m oligomers was analyzed by analytical SEC using a Superdex 200 10/300 GL column (GE Healthcare).

Crystallization and data collection. Crystals of the β_2m dimer were grown by vapor diffusion in hanging drops mixed from protein solution (10 mg ml^{-1}) with an equal amount of well solution. β_2m dimer was crystallized at 18 °C under the conditions of 0.1 mM MES, pH 6.2, 5% (w/v) PEG 3,000, 30% (w/v) PEG 200. Crystals were soaked in the cryoprotectant buffer containing the reservoir solution plus 25.0% (v/v) glycerol, followed by flash freezing. X-ray diffraction data were collected at 100 K at beamline 24-ID-C, Advanced Photon Source (APS), Argonne National Laboratory. Integration and scaling were done by using DENZO[55] and XSCALE[56]. The peptide segment LSFSKD was synthesized (Celtek Bioscience Peptides) and dissolved in water to 10 mg ml^{-1}. After hanging-drop vapor diffusion, thin needle-like crystals appeared in 0.1 M MMT buffer, pH 7.0, 25% (w/v) PEG 1,500. X-ray diffraction data were collected at 100 K at beamline 24-ID-E, APS. Statistics of data collection are listed in **Table 2**.

Structure determination. Wild-type monomeric β_2m (PDB ID code: 1LDS)[34] was used as a search model for molecular replacement with the program CNS[57]. Both rotation and translation searches gave convincing results. The model was subjected to simulated annealing in CNS. We used Coot[58] for model building and refined the model using transport-layer security (TLS) parameters implemented in REFMAC[59]. Coordinates were deposited with PDB ID code 3LOW.

For the segment LSFSKD, molecular replacement solutions were obtained using the program Phaser[60] with geometrically idealized β-strands as search models. Crystallographic refinement was done with the program REFMAC. Model building was done with Coot and illustrated with PyMOL (DeLano Scientific). Coordinates were deposited with PDB ID code 3LOZ.

Formation of oligomers and fibrils. For the wild-type β_2m protein, oligomerization and fibrillation were initiated upon incubation of 1 mg ml^{-1} monomeric or dimeric β_2m protein in aggregation buffer containing 5 mM DTT, 20 mM Tris-HCl, pH 8.0, at 37 °C without agitation. For SDS-PAGE analysis, DTT was removed before loading. Systematic screens for amyloidogenic segments were conducted by incubating 1, 5 and 10 mg ml^{-1} synthetic peptides in water or pH 2.0, 4.0, 7.0 buffers, with or without agitation at 37 °C.

Circular dichroism spectroscopy (CD). CD spectra were acquired using a JASCO J-715 spectrometer equipped with a JASCO PTC-348 temperature controller. Far-UV spectra (260–190 nm) were collected in 0.1-cm-path-length quartz cells with 20 μM β_2m in 20 mM Tris-HCl, pH 8.0. Near-UV spectra (320–250 nm) were recorded in 10-mm-path-length cells with 50 μM β_2m in 20 mM Tris-HCl, pH 8.0. All measurements were conducted at 23 °C. Raw data were processed by smoothing and subtraction of blank, according to the manufacturer's instructions.

Electron microscopy. Samples were spotted directly on freshly glow-discharged carbon-coated electron microscopy grids. After 3 min of incubation, grids were rinsed with distilled water and stained with 1% (w/v) uranyl formate solution. All images were taken by a Philips CM120 electron microscope at an accelerating voltage of 120 kV. Images were recorded digitally and at least two independent experiments were carried out for each sample.

Fibril X-ray diffraction. Wild-type β_2m was incubated in aggregation buffer at 37 °C for 60 d. Segments LSFSKD and KDWSFY were each incubated in water, with a final concentration of 5 mg ml^{-1}, at 37 °C with agitation for 20 d. After centrifuging, the pellets were rinsed with water, followed by resuspending in 5 μl of water, pipetting the suspension between two fire-polished glass rods and drying for 2–3 d. The sample was cooled to 100 K, and diffraction images were collected with 3 min exposures using a Rigaku FR-D X-ray generator equipped with an ADSC-Quantum4 CCD detector.

MALDI-TOF mass spectrometry. ^{15}N-labeled monomeric β_2m was mixed with native monomeric β_2m with a 1:1 molar ratio. Oligomer formation was accomplished by incubating the mixture in aggregation buffer at 37 °C for 3–30 d. Oligomers were further purified by Superdex 200 to exclude β_2m monomer and DTT. Purified oligomer samples were digested by sequencing-grade modified trypsin (Promega) with a molar ratio of 40:1 at 37 °C for 2.5 h.

MALDI-TOF mass spectra were acquired on a Voyager-DE STR Biospectrometry Workstation equipped with a nitrogen laser. Measurements were taken in the positive ion mode. Prior to MALDI MS analysis, samples were mixed with 0.5 μl of 10 mg ml^{-1} 2,5-dihydroxybenzoic acid (2,5-DHB) in water/acetonitrile (70:30, v/v) on a stainless-steel target plate and allowed to dry in a vacuum chamber. Data were collected in reflection mode using an accelerating voltage of 25 kV and a delay time of 200 ns. The accumulated spectra shown were obtained by 200–800 laser shots.

55. Otwinowski, Z. & Minor, W. Processing of X-ray diffraction data collected in oscillation mode. *Methods Enzymol.* **276**, 307–326 (1997).
56. Kabsch, W. Automatic processing of rotation diffraction data from crystals of initially unknown symmetry and cell constants. *J. Appl. Crystallogr.* **26**, 795–800 (1993).
57. Brünger, A.T. *et al.* Crystallography & NMR system: a new software suite for macromolecular structure determination. *Acta Crystallogr. D Biol. Crystallogr.* **54**, 905–921 (1998).
58. Emsley, P. & Cowtan, K. Coot: model-building tools for molecular graphics. *Acta Crystallogr. D Biol. Crystallogr.* **60**, 2126–2132 (2004).
59. Murshudov, G.N., Vagin, A.A. & Dodson, E.J. Refinement of macromolecular structures by the maximum-likelihood method. *Acta Crystallogr. D Biol. Crystallogr.* **53**, 240–255 (1997).
60. McCoy, A.J. *et al.* Phaser crystallographic software. *J. Appl. Crystallogr.* **40**, 658–674 (2007).

doi:10.1038/nsmb.1948